increases, the accuracy of size determinations increases and even smaller deletions are likely to be detected.

Finally, we compared BAC-CGH arrays, CNAT, and CNAG. BAC-arrays containing 3,151 FISH-mapped BAC/PAC clones with an average resolution of 1.0 Mb were constructed. The CRL-5929 cell line was examined using the BAC-array (Fig. 4*A*, *top*), CNAT (Fig. 4*A*, *middle*), and CNAG (Fig. 4*A*, *bottom*). The resolution on the SNP array allows for much finer mapping than BAC arrays, and additional compensations applied in CNAG provide more distinct copy number detection than CNAT. FISH analysis showed complete concordance with this method (Fig. 4*A*, *bottom*). This is more clearly seen in the immature T-cell line (HPB-ALL) on chromosome 2 (Fig. 4*B*). In this case, a homozygous deletion in 2p16.3 (*red arrow*) was detected by the 100K SNP array (Fig. 4*B*, *right*) but not detected by the BAC-array or CNAT (Fig. 4*B* (*left*), *top* and *bottom*, respectively). Lack of PCR product designed within the deleted region in HPB-ALL verified the deletion (Fig. 4*B*, *right*).

Allele-based copy number analysis. Another potential benefit from using a paired normal reference is the allele-based copy number analysis. In this approach, copy number estimates are done separately for each of the heterozygous SNPs (Fig. 5). The ratios can be separately defined for each of the alleles, grouped together into the larger (red) and smaller (green) ones and plotted in chromosomal order (Fig. 5; see Materials and Method). Although the analysis is confined to only heterozygous SNPs (mean heterozygosity of the Affymetrix GeneChip Mapping 100K SNPs is 0.29), it can effectively unmask regions showing copy neutral LOH due to genetic imbalances (asterisks in Fig. 5, *middle*), which are not detected by non-allele-based analysis (Fig. 5, *top*) or conventional BAC-array CGH.

Discussion

Recently, synthesized oligonucleotide microarrays have been used as alternatives to conventional BAC-array CGH for genome-wide copy number analysis (8–15). Large numbers of SNP markers are expected to enable ultra high-resolution copy number analysis; however, currently available algorithms do not take into account variation across different experiments, which can result in low S/N and high SD values. To address this problem, we developed a novelalgorithm for Affymetrix GeneChip Mapping 100K arrays, which includes robust compensations for systematic deviations of raw signal ratios across different experimental conditions and optimizes selection of the best-fit references. Together, these features effectively reduce heterogeneity between experiments and improve the SD value of log 2 ratios from 0.67 ± 0.12 to 0.18 ± 0.03, which is considerably lower than values reported for

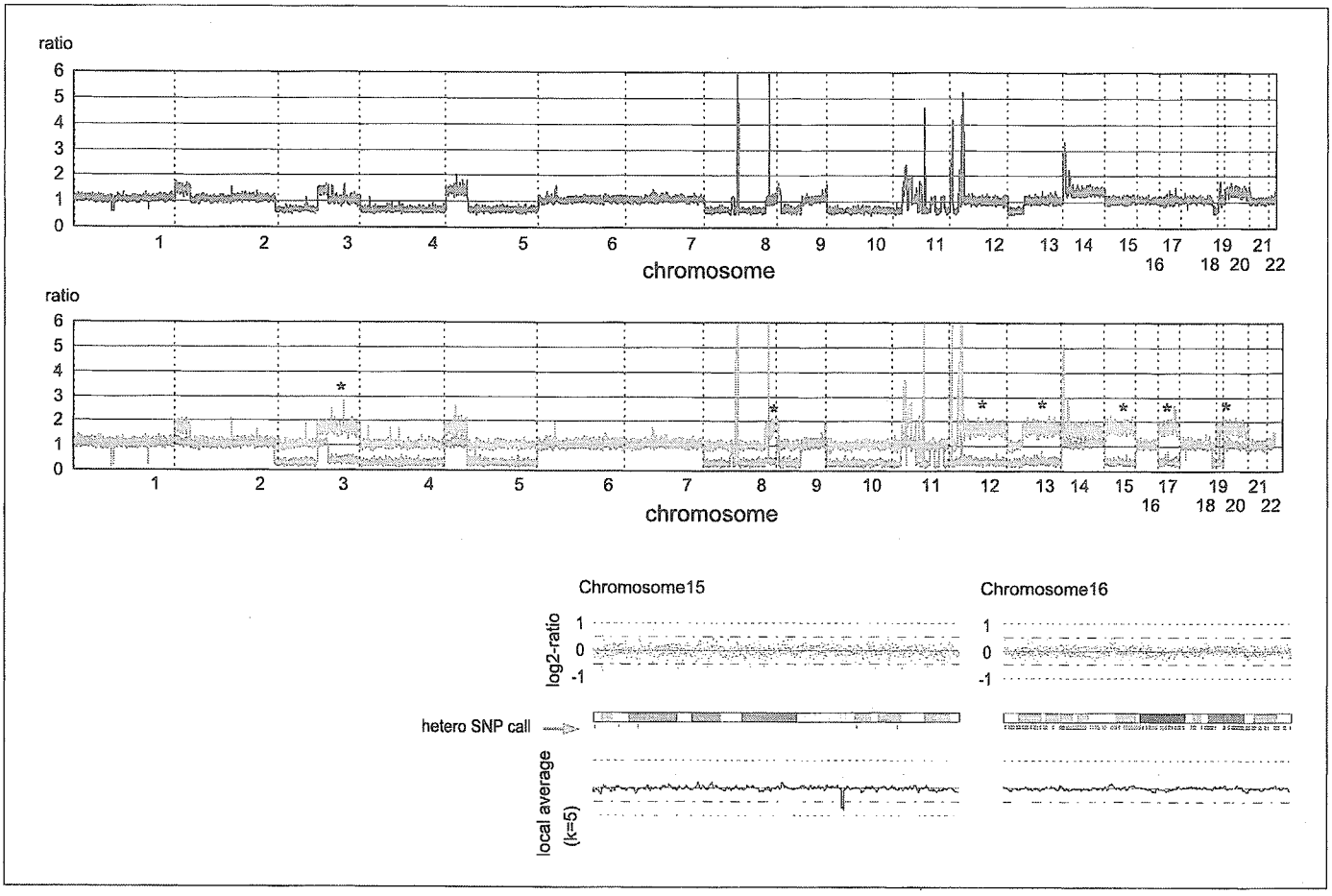

Figure 5. Copy number views of allele-based (*middle*) and non-allele-based analyses (*top* and *bottom*) of the same tumor samples as in Fig. 3 using the local mean analysis ($k = 5$). In the allele-based copy number view, the larger (Λ_{max}, *red lines*) and the smaller (Λ_{min}, *green lines*) log 2 ratios of the two log 2 ratios for allele A and allele B signals are separately grouped. Regions having copy neutral LOH as well as monosomy can be inferred from disappearance of heterozygous SNP calls in this non-allele-based analysis (*bottom*). Whereas no copy number changes are observed in both chromosomes 15 and 16, chromosome 15 shows copy neutral LOH as clearly seen in the allele-based copy number view (*middle*). Note that the existence of copy neutral LOH in chromosome 15 is inferred from the disappearance of heterozygous SNP calls in non-allele-based analysis (*bottom*).

oligonucleotide CGH-arrays (24). The SD value further decreases to 0.10 when log 2 ratios are locally averaged for consecutive five to ten SNPs (Fig. 2*C*). The reduction of SD values greatly contributes to high-quality copy number analysis across separately manipulated best-fit references.

Use of a paired normal reference further reduces SD values to 0.16 ± 0.03 ($P < 0.05$ for best-fit references), as comparison of signals is more accurately done between identical SNP loci. Use of a paired normal reference also enables allele-based analysis, which can unveil regions of copy neutral LOH in cancer cells. However, allele-based analysis only uses heterozygous SNPs, thus reducing the overall resolution by ~20% compared with the non-allele-based analysis. Recently, large regions with successive homozygous SNPs are reportedly commonly seen in leukemia samples (25).

Figure 2*C* illustrates that when a paired normal reference is unavailable, a best-fit reference can be used, resulting in SD reduction to 0.18 ± 0.03, which is only slightly higher than those obtained using a paired normal reference. In addition, the existence of copy neutral LOH can be also predicted from an unusually long tract of homozygous SNP calls in tumor samples (Fig. 5, *bottom*). Thus, when available, a paired normal reference is the ideal reference, but the average of the best-fit references is an excellent alternative that works satisfactorily in most cases, and at a lower cost.

The advantage of the copy number analysis using GeneChip Mapping 100K arrays over conventional BAC-array CGH lies in its extremely high resolution and availability of genotype information, enabling high-density LOH analysis. Although the number of BAC clones on a single array can vary from ~3,000 to ~32,000, there exists a clear limitation to their resolution because small deletions or gains relative to the size of the average BAC clones can easily escape detection in CGH analysis (Fig. 4*B*). Additional limitations include (*a*) requirement of large amounts of BAC genomic DNA for generating spotted arrays, a process which is difficult to quality control, and (*b*) lack of additional genotyping information indispensable for LOH detections. All of these challenges are overcome by Affymetrix GeneChip Mapping 100K arrays. These arrays are manufactured under stringent quality control procedures; the assay requires only 250 ng of starting genomic DNA per array and provides genotyping information at >99.5% accuracy. Together, these features comprise a comprehensive approach for copy number assessment at a resolution currently not achievable by other means.

This system also has limitations. For instance, polymorphism of primer locus or restriction site would affect the signal intensity that leads to misjudge of copy numbers. Although we can exclude these artifacts when these changes strides over different restriction fragments, validations using other methods are required to validate changes that are confined in a single fragment. It is sometimes difficult to distinguish deletions from large-scale copy number polymorphisms when best-fit references are used. In analyzing disease samples mixed with normal tissues, the amplitude of copy number changes diminishes according to the rate of normal fraction contamination. Whereas extensive SNP selection of the Mapping 100K arrays using >300 individuals likely resulted in the exclusion of SNPs on fragments with restriction site polymorphisms (via Hardy-Weinberg disequilibrium), we cannot exclude the possibility that rare mutations in restriction enzyme sites might affect amplification of affected fragments. Even if this did occur, it is highly unlikely to result in an erroneous copy number estimation because of the low likelihood that the mutation would affect more than one or two adjacent genomic fragments.

In conclusion, our improved copy number detection algorithm, combined with Affymetrix GeneChip Mapping 100K arrays, provides a powerful tool for high-resolution analysis of copy number alterations or variations across the human genome.

Acknowledgments

Received 2/14/2005; revised 4/11/2005; accepted 4/29/2005.

Grant support: Grants-in-Aid from Core Research for Evolutional Science and Technology of Japan Science and Technology Corporation; Research on Human Genome, Tissue Engineering, Ministry of Health, Labour, and Welfare; and Japan Health Science Foundation.

The costs of publication of this article were defrayed in part by the payment of page charges. This article must therefore be hereby marked *advertisement* in accordance with 18 U.S.C. Section 1734 solely to indicate this fact.

References

1. Albertson DG, Ylstra B, Segraves R, et al. Quantitative mapping of amplicon structure by array CGH identifies CYP24 as a candidate oncogene. Nat Genet 2000;25:144–6.
2. Hodgson G, Hager JH, Volik S, et al. Genome scanning with array CGH delineates regional alterations in mouse islet carcinomas. Nat Genet 2001; 29:459–64.
3. Pollack JR, Sorlie T, Perou CM, et al. Microarray analysis reveals a major direct role of DNA copy number alteration in the transcriptional program of human breast tumors. Proc Natl Acad Sci U S A 2002; 99:12963–8.
4. Iafrate AJ, Feuk L, Rivera MN, et al. Detection of large-scale variation in the human genome. Nat Genet 2004; 36:949–51.
5. Sebat J, Lakshmi B, Troge J, et al. Large-scale copy number polymorphism in the human genome. Science 2004;305:525–8.
6. Kallioniemi A, Kallioniemi OP, Sudar D, et al. Comparative genomic hybridization for molecular cytogenetic analysis of solid tumors. Science 1992;258: 818–21.
7. Ishkanian AS, Malloff CA, Watson SK, et al. A tiling resolution DNA microarray with complete coverage of the human genome. Nat Genet 2004;36: 299–303.
8. Bignell GR, Huang J, Greshock J, et al. High-resolution analysis of DNA copy number using oligonucleotide microarrays. Genome Res 2004;14:287–95.
9. Huang J, Wei W, Zhang J, et al. Whole genome DNA copy number changes identified by high density oligonucleotide arrays. Hum Genomics 2004; 4:287–99.
10. Janne PA, Li C, Zhao X, et al. High-resolution single-nucleotide polymorphism array and clustering analysis of loss of heterozygosity in human lung cancer cell lines. Oncogene 2004;23:2716–26.
11. Lieberfarb ME, Lin M, Lechpammer M, et al. Genome-wide loss of heterozygosity analysis from laser capture microdissected prostate cancer using single nucleotide polymorphic allele (SNP) arrays and a novel bioinformatics platform dChipSNP. Cancer Res 2003;63:4781–5.
12. Rauch A, Ruschendorf F, Huang J, et al. Molecular karyotyping using an SNP array for genomewide genotyping. J Med Genet 2004;41:916–22.
13. Wong KK, Tsang YT, Shen J, et al. Allelic imbalance analysis by high-density single-nucleotide polymorphic allele (SNP) array with whole genome amplified DNA. Nucleic Acids Res 2004;32:e69.
14. Zhao X, Li C, Paez JG, et al. An integrated view of copy number and allelic alterations in the cancer genome using single nucleotide polymorphism arrays. Cancer Res 2004;64:3060–71.
15. Zhou X, Cole SW, Hu S, Wong DT. Detection of DNA copy number abnormality by microarray expression analysis. Hum Genet 2004;114:464–7.
16. Fodor SP, Read JL, Pirrung MC, Stryer L, Lu AT, Solas D. Light-directed, spatially addressable parallel chemical synthesis. Science 1991;251:767–73.
17. Pease AC, Solas D, Sullivan EJ, Cronin MT, Holmes CP, Fodor SP. Light-generated oligonucleotide arrays for rapid DNA sequence analysis. Proc Natl Acad Sci U S A 1994;91:5022–6.
18. Kennedy GC, Matsuzaki H, Dong S, et al. Large-scale genotyping of complex DNA. Nat Biotechnol 2003;21:1233–7.
19. Matsuzaki H, Dong S, Loi H, et al. Genotyping over 100,000 SNPs on a pair of oligonucleotide arrays. Nat Methods 2004;1:109–11.
20. Lin M, Wei LJ, Sellers WR, Lieberfarb M, Wong WH, Li C. dChipSNP: significance curve and clustering of SNP-array-based loss-of-heterozygosity data. Bioinformatics 2004;20:1233–40.
21. Rakesh Dugad, Desai UB. A tutorial on Hidden Markov Models. No. SPANN-96.1, 1996. p. 1–16.
22. Rajagopalan H, Lengauer C. Aneuploidy and cancer. Nature 2004;432:338–41.
23. Hans GD. The leukemia-lymphoma cell line facts book. London: Academic Press; 2001. p. 371–2.
24. Carvalho B, Ouwerkerk E, Meijer GA, Ylstra B. High resolution microarray comparative genomic hybridisation analysis using spotted oligonucleotides. J Clin Pathol 2004;57:644–6.
25. Raghavan M, Lillington DM, Skoulakis S, et al. Genome-wide single nucleotide polymorphism analysis reveals frequent partial uniparental disomy due to somatic recombination in acute myeloid leukemias. Cancer Res 2005;65:375–8.

GENES, CHROMOSOMES & CANCER 42:269–279 (2005)

Identification of a SRC-Like Tyrosine Kinase Gene, *FRK*, Fused with *ETV6* in a Patient with Acute Myelogenous Leukemia Carrying a t(6;12)(q21;p13) Translocation

Noriko Hosoya,[1] Ying Qiao,[1] Akira Hangaishi,[1] Lili Wang,[1] Yasuhito Nannya,[1] Masashi Sanada,[1] Mineo Kurokawa,[1] Shigeru Chiba,[1,2] Hisamaru Hirai,[1,2] and Seishi Ogawa[1,3]*

[1]Department of Hematology and Oncology, Graduate School of Medicine, University of Tokyo, Tokyo, Japan
[2]Department of Cell Therapy and Transplantation Medicine, University of Tokyo Hospital, University of Tokyo, Tokyo, Japan
[3]Department of Regeneration Medicine for Hematopoiesis, Graduate School of Medicine, University of Tokyo, Tokyo, Japan

The SRC family of kinases is rarely mutated in primary human tumors. We report the identification of a SRC-like tyrosine kinase gene, *FRK* (Fyn-related kinase), fused with *ETV6* in a patient with acute myelogenous leukemia carrying t(6;12)(q21;p13). Both reciprocal fusion transcripts, *ETV6/FRK* and *FRK/ETV6*, were expressed. In *ETV6/FRK*, exon 4 of *ETV6* was fused in-frame to exon 3 of *FRK*, producing a chimeric protein consisting of the entire oligomerization domain of ETV6 and the kinase domain of FRK. The ETV6/FRK protein was shown to be constitutively autophosphorylated on its tyrosine residues. ETV6/FRK phosphorylated histones H2B and H4 in vitro to a greater extent than did FRK, suggesting it had elevated kinase activity. ETV6/FRK could transform both Ba/F3 cells and NIH3T3 cells, which depended on its kinase activity. Moreover, ETV6/FRK inhibited ETV6-mediated transcriptional repression in a dominant-negative manner. This report provides the first evidence that a SRC-like kinase gene, *FRK* fused with *ETV6*, could directly contribute to leukemogenesis by producing an oncoprotein, ETV6/FRK, with dual functions: constitutive activation of the ETV6/FRK tyrosine kinase and dominant-negative modulation of ETV6-mediated transcriptional repression.

INTRODUCTION

The *SRC* gene was the first protooncogene isolated as the cellular homologue of v-*SRC*, the retroviral transforming oncogene of avian Rous sarcoma virus (Brown and Cooper, 1996). Since then, it has become clear that *SRC* is the prototype for a family of genes that encode nonreceptor tyrosine kinases implicated in a variety of cellular processes, including cell growth, differentiation, and carcinogenesis. The SRC family of kinases shares common structures consisting of an N-terminal unique domain, SRC homology 3 (SH3) and SRC homology 2 (SH2) domains, a kinase domain, and a short C-terminal regulatory tail (Brown and Cooper, 1996). They are normally maintained in an inactive state through phosphorylation of a critical C-terminal tyrosine residue (Tyr 530 in human SRC, Tyr 527 in chicken SRC) by the C-terminal SRC kinase (Csk) (Brown and Cooper, 1996). The SH3 and SH2 domains also participate in this negative regulation through intramolecular interactions (Brown and Cooper, 1996; Schindler et al., 1999; Xu et al., 1999; Young et al., 2001).

The SRC and its family member kinases have long been postulated to participate in oncogenic processes. Activated variants of SRC family kinases, including the viral oncoprotein v-SRC, are capable of inducing malignant transformation in a variety of cell types (Parker et al., 1984; Cartwright et al., 1987). Activation of SRC-like kinases recently was described in *BCR-ABL1*-expressing acute lymphoblastic leukemia in mice (Hu et al., 2004). Elevated expression and/or activity of SRC have been documented in several types of primary human tumors (Bolen et al., 1987; Ottenhoff-Kalff et al., 1992; Talamonti et al., 1993). However, for many years, structural abnormalities of the SRC family of kinases have been detected rarely in primary human tumors. Although Irby et al. (1999)

Supported by: Research on Human Genome and Tissue Engineering, Health and Labour Sciences Research Grants, Ministry of Health, Labour and Welfare of Japan; Japan Society for the Promotion of Science; Grant number: KAKENHI 14570962.

*Correspondence to: Seishi Ogawa, Department of Hematology and Oncology, Department of Regeneration Medicine for Hematopoiesis, Graduate School of Medicine, University of Tokyo, 7-3-1, Hongo, Bunkyo-ku, Tokyo 113-8655, Japan.
E-mail: sogawa-tky@umin.ac.jp

Received 22 July 2004; Accepted 15 October 2004
DOI 10.1002/gcc.20147
Published online 20 December 2004 in Wiley InterScience (www.interscience.wiley.com).

reported that 12% of advanced human colon cancers had a truncating mutation at codon 531 of the *SRC* gene, determining the importance of this mutation in the generation of colorectal cancers remained elusive according to the negative results in subsequent reports (Daigo et al., 1999; Wang et al., 2000; Laghi et al., 2001). In primary hematopoietic malignancies, no studies have demonstrated structural abnormalities of the SRC family of kinases.

In this study, we performed molecular analysis of a t(6;12)(q21;p13) observed as the sole chromosomal abnormality in a case of acute myelogenous leukemia (AML) and identified a SRC-like tyrosine kinase gene, *FRK* (Fyn-related kinase or *Rak*), on 6q21 (Cance et al., 1994; Lee et al., 1994) that is fused with *ETV6* (also called *TEL*), a gene frequently involved in chromosomal translocations in a variety of human leukemias (Golub et al., 1997). We found that the resultant chimeric protein, ETV6/FRK, is a transforming oncoprotein with elevated kinase activity. We also demonstrated that ETV6/FRK inhibits ETV6-mediated transcriptional repression in a dominant-negative manner, indicating that ETV6/FRK is a unique oncoprotein with dual functions. This is the first report showing the involvement of a SRC-like kinase gene (*FRK*) in primary human cancers.

MATERIALS AND METHODS

Case History

The patient was a 69-year-old Japanese woman with AML-M4, carrying the translocation t(6;12)(q21;p13) as the sole chromosomal abnormality in 8 of 20 examined bone marrow metaphase cells. After obtaining informed consent, a sample of her bone marrow was taken for use in this study. The patient did not respond to chemotherapy and died 5 months later.

Fluorescence In Situ Hybridization Analysis

Fluorescence in situ hybridization (FISH) analysis was performed as previously described (Pinkel et al., 1986) with a panel of biotin- and digoxigenin-labeled cosmid probes that contained different exons of *ETV6*, kindly provided by Dr. Peter Marynen (University of Leuven, Leuven, Belgium). The order and the relative locations of cosmids are depicted in Figure 1A.

3′-Rapid Amplification of cDNA End

To do the 3′-rapid amplification of cDNA end (RACE), total RNA was isolated from the leukemic sample as described previously (Ogawa et al., 1996). First-strand cDNA was synthesized from 2.5 μg of total RNA using the primer R2N6 as described previously by Peeters et al. (1997). The first polymerase chain reaction (PCR) was performed with primers T4F1 and R2N6R1 (Peeters et al., 1997). Then, a diluted product of the first PCR, along with primers T4F2 and R2N6R2, was used for the second, nested PCR (Peeters et al., 1997). The nucleotide sequences of the primers used in this study and the conditions for PCR are listed in Table 1. The PCR products were subcloned into the pCR® 2.1-TOPO® vector using a TOPO TA Cloning® kit (Invitrogen, Tokyo, Japan) and subjected to DNA sequencing by use of a 3100 Applied Biosystems automated sequencer (Applied Biosystems, Chiba, Japan).

Reverse Transcriptase–PCR

For the reverse transcriptase-PCR (RT-PCR), 5 μg of the total RNA was transcribed to cDNA with 2 units of Moloney murine leukemia virus reverse-transcriptase (MMLV-RT, Stratagene, La Jolla, CA) using a random hexamer. One-tenth of the synthesized cDNA was directed to PCR analysis. Primers T4F2 and FRK1198R were used to confirm the *ETV6/FRK* transcripts. The primers for detecting the reciprocal *FRK/ETV6* transcripts were FRK451F and TEL723R. For amplification of the wild-type *ETV6* and *FRK* transcripts, primers T4F2 and TEL723R and primers FRK808F and FRK1198R, respectively, were used. All the sequences of the RT-PCR products were verified by direct sequencing.

Plasmid Construction

Full-length *ETV6* cDNA tagged with a FLAG sequence at the 5′ end, a gift from Dr. Kinuko Mitani (Dokkyo University School of Medicine, Tochigi, Japan), was subcloned into the expression plasmid pME18S-neo (Invitrogen, San Diego, CA). A FLAG-tagged full-length *FRK* cDNA was isolated by RT-PCR from total RNA obtained from human placenta using primers *Eco*RI-FLAG-FRK and FRK-*Not*I-2058R and was cloned into pME18S-neo. The pME18S-neo-FLAG-ETV6/FRK vector was generated by replacement of the *Cla*I-*Not*I fragment of the pME18S-neo-FLAG-ETV6 vector with the *Cla*I-*Not*I fragment of *ETV6/FRK*, which was obtained by RT-PCR from the patient's bone marrow using primers TEL-*Cla*I-F and FRK-*Not*I-2058R, with subsequent digestion with *Cla*I and *Not*I. To construct a kinase-inactive mutant of ETV6/FRK, designated ETV6/FRK(K262R), a point mutation corresponding

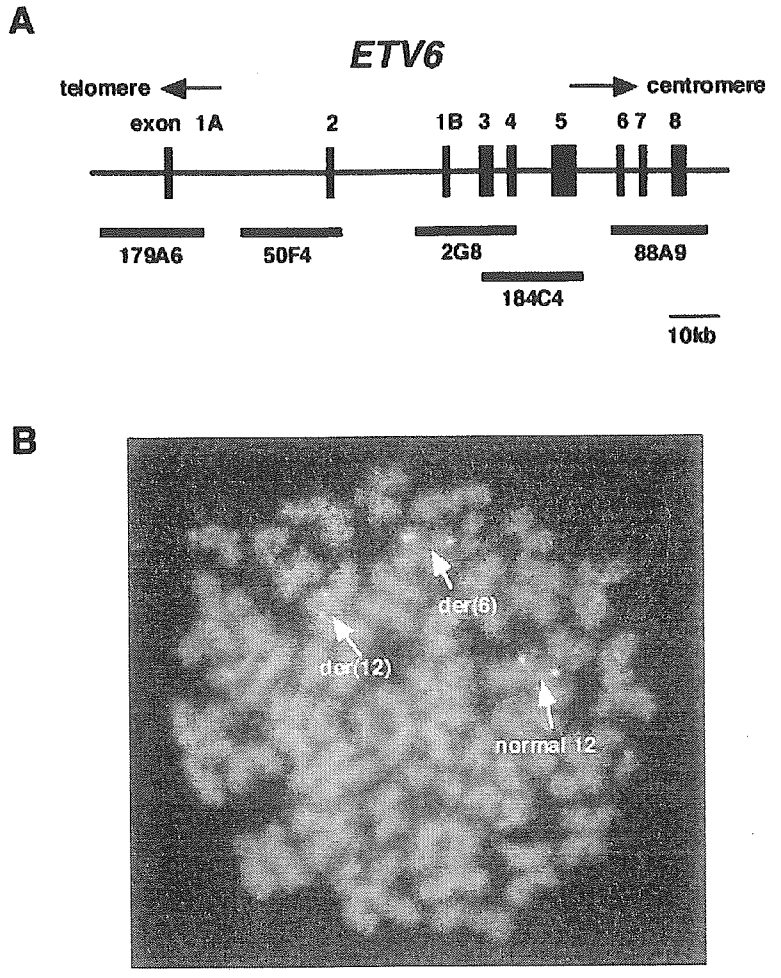

Figure 1. Analysis of breakpoint on chromosome 12. (A) A genomic map of *ETV6* and location of the cosmid probes used for FISH analysis. (B) FISH analysis of the patient's leukemic cells. The signals of the 2G8 probe (red) containing *ETV6* exons 1B, 3, and 4 are hybridized on the der(6) and on the normal 12p, whereas those of the 184C4 probe (green) containing *ETV6* exons 3–5 are found on the der(6), the der(12), and the normal 12p.

to a kinase-inactivating mutation in the ATP-binding site lysine residue (Lys262) of FRK was introduced into *ETV6/FRK* cDNA. A mutated fragment generated by PCR using the mutagenic primer FRK-K262R-*Bam*HI and the primer TEL-*Eco*RI-FLAG was spliced together with a C-terminal partial fragment of *FRK* into pME18S-neo. A FLAG-tagged full-length *FRK/ETV6* cDNA was constructed into the pME18S-neo vector by assembling partial fragments from *ETV6* and *FRK* and a fragment spanning the *FRK/ETV6* junction generated by RT-PCR using primers FRK451F and TEL723R. All the constructs were sequenced to confirm the fidelity of the sequence and conservation of the reading frame at the site of fusion.

Cell Lines, Transfection, and Cell Transformation Studies

For transient expression studies, 4×10^4 HeLa cells were seeded in each 60-mm dish and transfected with expression plasmid or plasmids 24 hr later by a lipofection method using Effectine™ Transfection Reagent (Qiagen, Hilden, Germany). Cells were incubated for 48 hr and harvested for analysis. NIH3T3 cells were transfected with expression plasmids, also using Effectine™, and selected in 400 μg/ml of G418 for 2 weeks. Ba/F3 clones stably expressing ETV6/FRK or other proteins were obtained by electroporation of each expression plasmid into Ba/F3 cells as previously described (Carroll et al., 1996) and subsequent isolation of individual G418-resistant subclones by limiting dilution. Expression of the transfected genes was evaluated by immunoblotting as previously described (Maki et al., 1999) using anti-FLAG-M2 monoclonal antibody (Sigma-Aldrich, St. Louis, MO). The soft-agar colony assay was performed as previously described (Kurokawa et al., 1996). After 21 days, all macroscopic colonies larger than 0.25 mm in diameter were counted. For growth curves, 2×10^4 G418-resistant Ba/F3 cells were washed 3 times with PBS and plated in IL-3-free medium on day 0, and viable cells were counted each day by trypan blue exclusion.

TABLE I. Primers Used For 3′-RACE and (RT)-PCR Amplifications

Name	Sequence
R2N6	5′-CCAGTGAGCAGAGTGACGAGGACTCGAGCTCAAGC(N)6-3′
T4F1	5′-CATATTCTGAAGCAGAGGAAA-3′
R2N6R1	5′-CCAGTGAGCAGAGTGACG-3′
T4F2	5′-ACACAGCCGGAGGTCATACT-3′
R2N6R2	5′-GAGGACTCGAGCTCAAGC-3′
FRK1198R	5′-CTTCCCATACTTCGCAAAC-3′
FRK451F	5′-AGCAACATCTGTCAGAGGCT-3′
TEL723R	5′-GTAGGACTCCTGGTGGTTGTT-3′
FRK808F	5′-ATCGGAAGATCAGATGCAGAG-3′
*Eco*RI-FLAG-FRK	5′-GCGAATTCGTTGTGATGGGGGACTACAAGGACGAC GATGACAAGTCCGGGAGCAACATCTGTCAGAGGCT-3′
FRK-*Not*I-2058R	5′-ATTGCGGCCGCACTGATTGTGCAGTTGGTTGA-3′
TEL-*Cla*I-F	5′-CTTTCGCTATCGATCTCCTCA-3′
TEL-*Eco*RI-FLAG	5′-GCGAATTCGTTGTGATGGGGGACTACAAGGACGAC GATGACAAGTCCGGGTCTGAGACTCCTGCTCAGTG-3′
FRK-K262R-*Bam*HI	5′-TTGGATCCATTGAACCTGGTTTTAATGTTCTCACTG-3′

Thermal cycling profile was: 94°C for 2 min, followed by 35 cycles of 94°C for 1 min, 60°C for 1 min and 72°C for 2 min, with a final extension at 72°C for 10 min.

Immunoprecipitation, Immunoblotting, and Immune Complex Kinase Assay

Lysates were prepared by washing cells (1×10^6–1×10^7) with phosphate-buffered saline and then adding lysis buffer [10 mM Tris-HCl (pH 7.4), 150 mM NaCl, 1.0% NP-40, 1 mM EDTA, and 1 mM Na3VO4] containing 5 mM phenylmethyl-sulfonylfluoride and 1 μg/ml of aprotinin. After 10 min on ice, the samples were centrifuged at 12,000 g to remove insoluble particles. For immunoprecipitation, 1 mg of total cell lysate was incubated with anti-FLAG-M2 antibody for 1 hr at 4°C, after which 50 μl of Protein G-Sepharose beads (Amersham Biosciences, Uppsala, Sweden) was added. After rotating for 1 hr at 4°C, immunoprecipitates were washed 3 times and boiled in loading buffer for 5 min. Protein samples were separated on 6.5%–15% gradient SDS-polyacrylamide gels and transferred onto PVDF membranes (Millipore, Bedford, MA). Immunoblotting was performed as previously described (Maki et al., 1999) using either anti-FLAG-M2 antibody or antiphosphotyrosine monoclonal antibody 4G10 (Upstate Biotechnology Incorporated, Lake Placid, NY) as a primary antibody.

For the immune complex kinase assay, immunoprecipitates were washed 3 times and suspended in kinase buffer [40 mM HEPES (pH 7.4), 10 mM $MgCl_2$, 5 mM $MnCl_2$]. For determination of kinase activity, 2.5 μg of either histone H2B or histone H4 (Roche Diagnostics K. K., Tokyo, Japan) was added to each reaction. Kinase reactions were initiated by the addition of 10 μCi of [γ-^{32}P] ATP (3,000 Ci/mmol; Amersham Biosciences Corp., Piscataway, NJ) and incubated at 30°C for 15 min. Reactions were stopped by the addition of loading buffer and analyzed by SDS-PAGE and exposure to a film.

Luciferase Assay

For the luciferase assay, 4×10^4 HeLa cells were transfected with 1 μg of the reporter plasmid (EBS)3tkLuc (Waga et al., 2003), a kind gift of Dr. Kinuko Mitani, along with the indicated amounts of the expression vectors. The total amount of DNA in weight was adjusted to be equal by adding pME18S-neo plasmid. Luciferase activities were determined as described previously (Maki et al., 1999). All transfection experiments were performed in duplicate at least 3 times.

RESULTS

Identification of the Breakpoint on Chromosome 12

We performed FISH experiments using several probes from the *ETV6* locus, on 12p13 (Fig. 1A). The signals from the cosmids containing exons 1–4 (179A6, 50F4, and 2G8) were found on the der(6) (Fig. 1B), whereas the signals from the cosmid containing exons 3–5 (184C4) were split to the der(6) and the der(12) (Fig. 1B), suggesting that the breakpoint on 12p13 was localized to *ETV6* exons 4–5. The signals on the normal 12p were always observed with all the indicated cosmid probes of the *ETV6* locus, suggesting that the non-

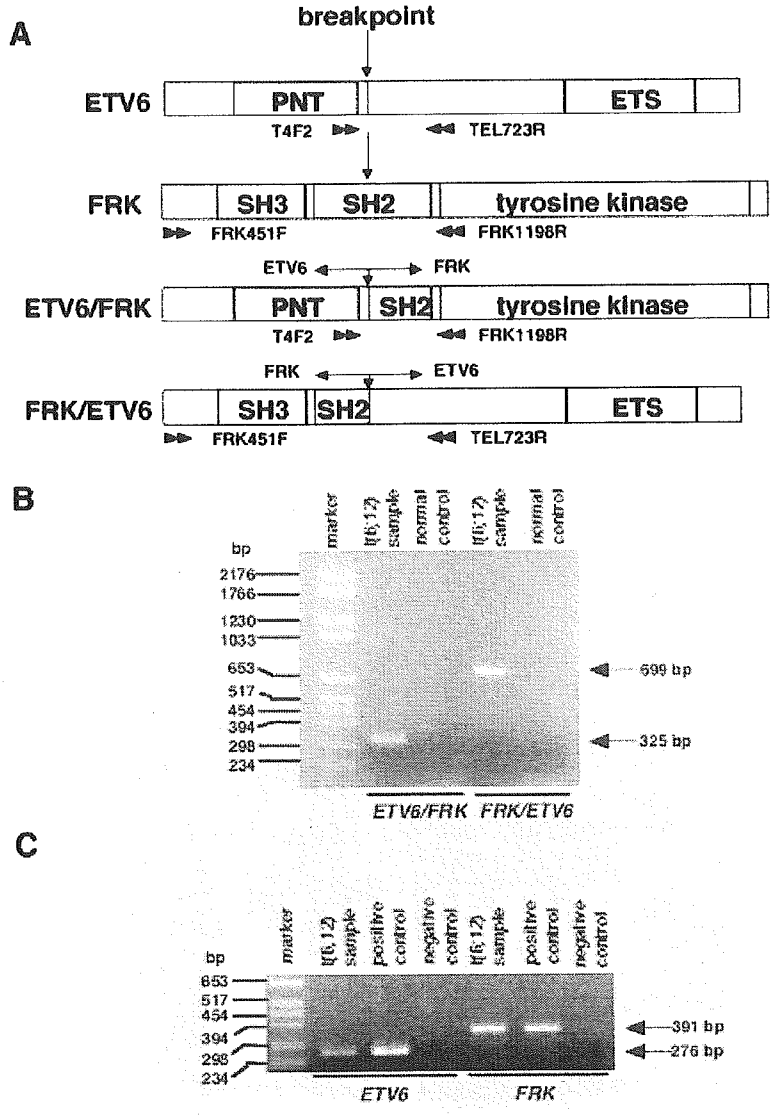

Figure 2. Identification of *ETV6/FRK* and *FRK/ETV6* fusion transcripts. (A) Schematic representation of wild-type *ETV6*, *FRK*, and the fusion transcripts. The breakpoints are indicated by vertical arrows. Horizontal arrows indicate the positions of RT-PCR primers (described in the Materials and Methods section). (B) Detection of *ETV6/FRK* as well as *FRK/ETV6* fusion transcripts by RT-PCR in the patient's leukemic sample. (C) Expression of *ETV6* and *FRK* in the patient's leukemic sample by RT-PCR.

translocated allele of *ETV6* was grossly intact with no large deletions.

Identification of the Fusion Partner of *ETV6*

To identify the unknown fusion partner of *ETV6*, 3′-RACE-PCR was performed. After two rounds of PCR, 3′-RACE-PCR products were successfully obtained. Sequencing analysis of the PCR products showed that exon 4 of *ETV6* was fused to exon 3 of *FRK* on 6q21, creating an *ETV6/FRK* fusion gene. The *FRK* gene encodes a SRC-like nonreceptor tyrosine kinase, consisting of the N-terminal SH3 and SH2 domains, the C-terminal kinase domain, and a short regulatory tail (Fig. 2A). The *ETV6/FRK* fusion gene produced a chimeric protein in which the entire pointed (PNT) oligomerization domain (also called helix–loop–helix domain) of ETV6 and the kinase domain of FRK were fused in-frame (Fig. 2A).

Detection of the *ETV6/FRK* and *FRK/ETV6* Fusion Transcripts

RT-PCR analysis was performed to confirm the fusion transcripts of the *ETV6* and *FRK* genes. Both reciprocal fusion transcripts, *ETV6/FRK* and *FRK/ETV6*, were specifically amplified from the leukemic sample but not from control bone marrow (Fig. 2B). Expression of wild-type *ETV6* and *FRK* also was detected in the leukemic sample (Fig. 2C). There were no mutations in the entire coding sequences of *ETV6*, *FRK*, *ETV6/FRK*, and *FRK/ETV6* (data not shown).

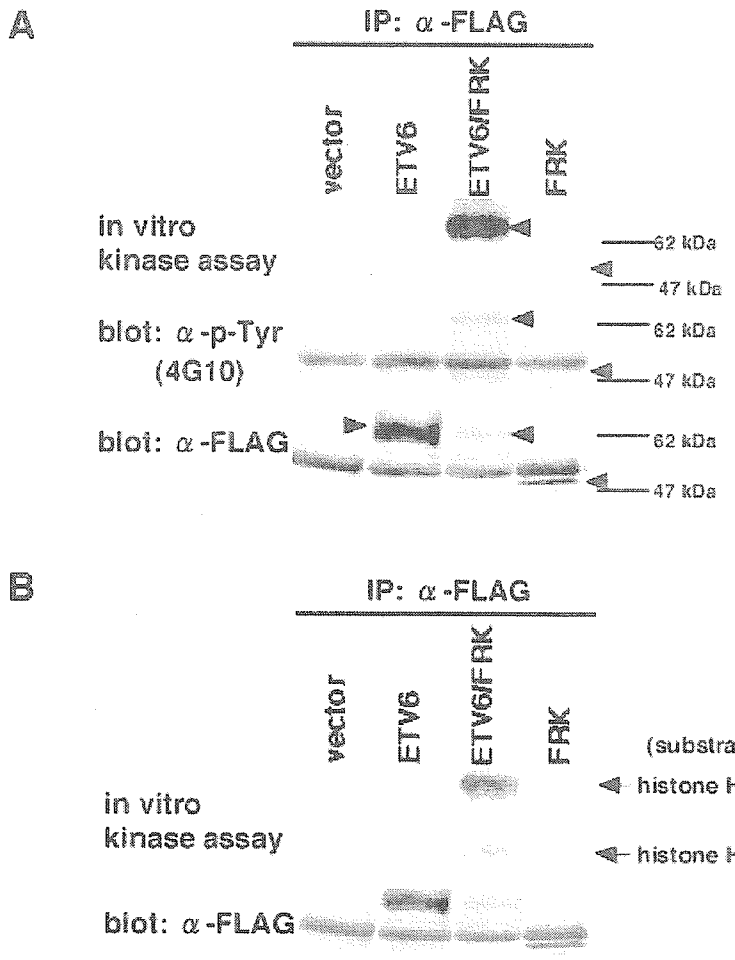

Figure 3. The ETV6/FRK tyrosine kinase is constitutively activated in HeLa cells. (A) Lysates of HeLa cells transfected with the indicated expression vectors were immunoprecipitated with an anti-FLAG-M2 monoclonal antibody and then analyzed by immune complex kinase assay (top) or immunoblotting with an antiphosphotyrosine antibody 4G10 (middle). The total amount of each protein was also assessed by immunoblotting with anti-FLAG-M2 antibody (bottom). Arrowheads show the proteins expressed or phosphorylated at an expected size. (B) Results of kinase assay performed with histones H2B (top) and H4 (middle).

Constitutive Activation of the ETV6/FRK Tyrosine Kinase

Because the ETV6/FRK fusion protein retained the kinase domain but lacked the SH3 domain and most of the SH2 domain, we examined its kinase activity. First, we compared the autophosphorylation status of ETV6/FRK and wild-type FRK. Either the ETV6/FRK fusion protein, wild-type FRK, or wild-type ETV6 FLAG-tagged at the N-terminus was introduced into HeLa cells, immunoprecipitated with an anti-FLAG-M2 monoclonal antibody, and then analyzed by the kinase assay or immunoblotting with an antiphosphotyrosine antibody 4G10 (Fig. 3A, top and middle). To compare expression levels, the same amounts of immunoprecipitate were also subjected to anti-FLAG blot (Fig. 3A, bottom). A high level of tyrosine phosphorylation occurred only in the ETV6/FRK protein (Fig. 3A, top and middle). A basal level of autophosphorylation also was detectable in the wild-type FRK (Fig. 3A, top), a finding in agreement with the previous data (Cance et al., 1994). However, the level of autophosphorylation was significantly lower than that of ETV6/FRK (Fig. 3A, top and middle). Next, we compared the ability of ETV6/FRK and wild-type FRK to phosphorylate exogenous substrates. When histone H2B or H4 was added to the kinase reaction, they were found to be phosphorylated to a greater extent in ETV6/FRK-expressing cells than in FRK-expressing cells (Fig. 3B), suggesting that the ETV6/FRK protein had elevated tyrosine kinase activity.

Cell Transformation by ETV6/FRK in a Kinase-Dependent Manner

To assay the transforming activities of ETV6/FRK, we stably expressed the cDNA-encoding ETV6/FRK or other proteins into the fibroblast cell line NIH3T3. We established 3 NIH3T3 clones expressing ETV6/FRK, 2 clones expressing FRK/ETV6, 2 clones expressing FRK, 2 clones expressing ETV6, and 2 clones expressing ETV6/FRK(K262R) (Fig. 4A), the kinase-inactive

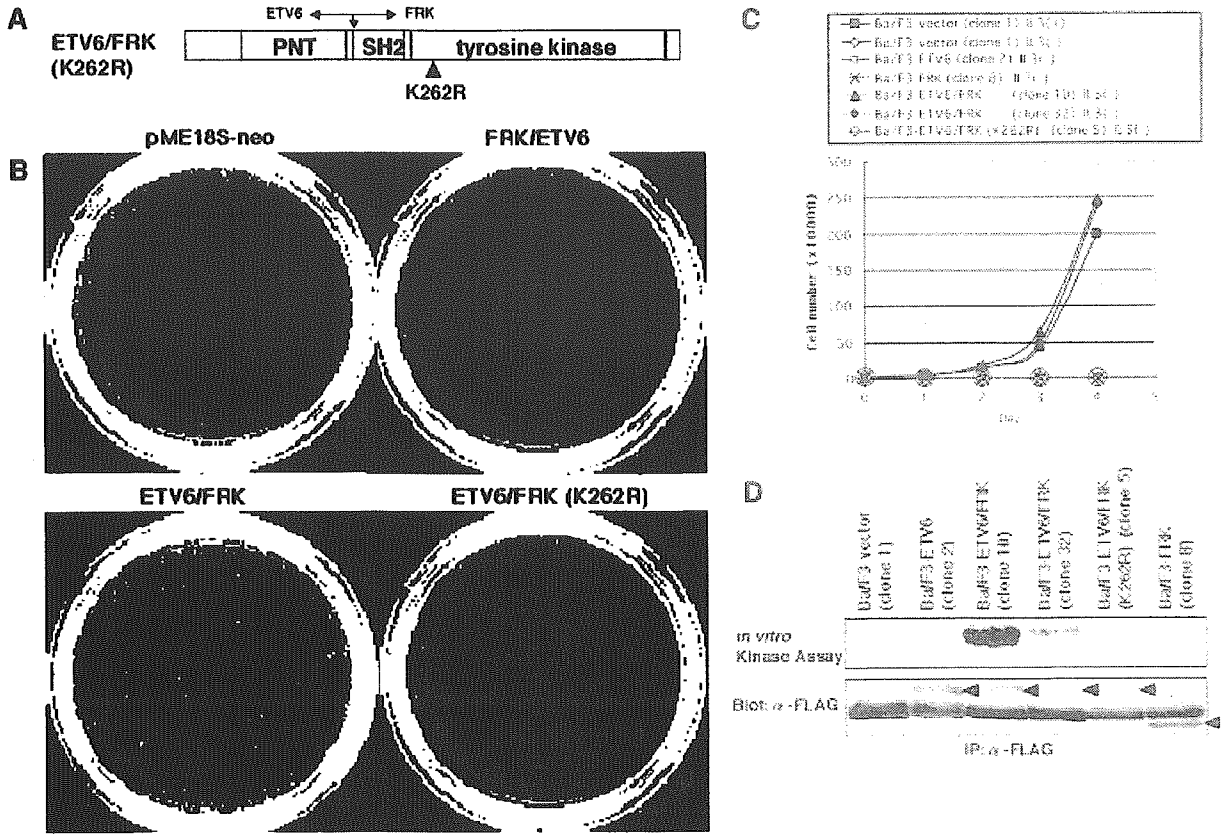

Figure 4. ETV6/FRK transforms NIH3T3 cells and Ba/F3 cells in a kinase-dependent manner. (A) Schematic representation of the kinase-inactive ETV6/FRK(K562R) mutant with a lysine-to-arginine mutation at the ATP binding site. (B) Soft-agar assay demonstrating macroscopic colony formation in ETV6/FRK-expressing NIH3T3 cells. (C) 2 × 10^4 Ba/F3 cells stably transfected with the indicated expression vectors were washed free of IL-3 and plated on day 0 in growth medium without IL-3. Viable cells were counted each day. Data of the representative clone(s) for each protein are presented. (D) Cell lysates of the indicated Ba/F3 clones were immunoprecipitated with an anti-FLAG-M2 antibody and then subjected to kinase assay (top) and immunoblotting with anti-FLAG-M2 antibody (bottom). Arrowheads show the proteins expressed at an expected size.

mutant of ETV6/FRK, confirmed by immunoblotting analysis (data not shown). The soft-agar assay was performed on each clone. Comparable results were obtained for the clones expressing the same proteins, and the representative data are presented. Only the NIH3T3 cells expressing intact ETV6/FRK were able to produce macroscopic colonies, whereas the NIH3T3 cells transfected with the empty vector or cells expressing the kinase-inactive mutant ETV6/FRK(K262R), the reciprocal FRK/ETV6 fusion protein, wild-type FRK, or wild-type ETV6 failed to grow colonies (Fig. 4B, Table 2). These results suggest that ETV6/FRK but not FRK/ETV6 contributes to neoplastic transformation in a kinase-dependent manner.

Next, we also examined the ability of ETV6/FRK to transform the murine hematopoietic cell line Ba/F3, which is strictly dependent on IL-3 for survival and proliferation. Following stable transduction by electroporation, we obtained 6 Ba/F3 clones expressing ETV6/FRK, 2 clones expressing FRK, 2 clones expressing ETV6, and 3 clones expressing ETV6/FRK(K262R), confirmed by immunoblotting analysis (data not shown). To assay the ability to confer independent proliferation of IL-3, each Ba/F3 clone was switched to growth medium without IL-3. Comparable results were obtained for the clones expressing the same proteins, and the representative data are presented. The Ba/F3 clones expressing ETV6/FRK showed sustained proliferation in the absence of IL-3 (Fig. 4C). In contrast, Ba/F3 cells transfected with the empty vector or cells expressing kinase-inactive mutant ETV6/FRK(K262R), wild-type FRK, and wild-type ETV6 were all unable to proliferate in the absence of IL-3 (Fig. 4C). Although the ETV6/FRK proteins expressed in the stable clones were constitutively autophosphorylated, the ETV6/FRK(K262R) mutants were not (Fig. 4D). These observations indicate that ETV6/FRK is a dominant oncoprotein and that constitutive activa-

TABLE 2. Transformation of NIH3T3 Cells By ETV6/FRK

Transfected DNA	No. of colonies[a]
pME18S-neo (vector)	0
pME18S-neo-ETV6	0
pME18S-neo-FRK	0
pME18S-neo-ETV6/FRK	15
pME18S-neo-ETV6/FRK(K262R)	0
pME18S-neo-FRK/ETV6	0

NIH3T3 cells were transfected with the indicated constructs, and stable transfectants were selected in G418. Cells were plated in soft agar. Macroscopic colonies were counted at day 21.
[a]Average of four experiments.

tion of the ETV6/FRK tyrosine kinase is necessary for ETV6/FRK-induced transformation.

Inhibition of ETV6-Mediated Transcription Repression by ETV6/FRK

Because ETV6 is an ETS transcription factor that acts as a transcriptional repressor (Lopez et al., 1999), we also investigated the transcriptional regulatory property of ETV6/FRK and its ability to modulate the function of wild-type ETV6. We transfected a previously described (EBS)3tkLuc reporter, in which the luciferase gene is placed under the control of an ETS responsive promoter (Waga et al., 2003), along with either wild-type ETV6, ETV6/FRK, or FRK/ETV6 into HeLa cells and evaluated luciferase activity. The results showed, in agreement with the previous finding (Waga et al., 2003), that there was decreased luciferase activity after cotransfection of (EBS)3tkLuc with the wild-type ETV6 expression plasmid (Fig. 5A). In contrast, no repression was observed when ETV6/FRK or FRK/ETV6 was expressed with the (EBS)3tkLuc reporter (Fig. 5A).

Because the oncoprotein ETV6/FRK lacks the ETS DNA binding site but still retains the PNT oligomerization domain, it is possible that it might affect ETV6-mediated transcriptional repression by heterodimerizing with ETV6. Notably, coexpression of ETV6/FRK abolished the transcriptional repression by ETV6 in a dose-dependent manner (Fig. 5B), suggesting that ETV6/FRK has a dominant-negative effect on ETV6-mediated transcriptional repression. In contrast, coexpression of the reciprocal FRK/ETV6 protein did not affect ETV6-mediated transcriptional repression (Fig. 5B). In control experiments, dose-dependent expression of the ETV6, ETV6/FRK, or FRK/ETV6 protein was confirmed by immunoblotting analysis (data not shown).

DISCUSSION

The t(6;12)(q21;p13) is a rare but recurrent reciprocal chromosome translocation in human leukemia (Hayashi et al., 1990; Katz et al., 1991; Raimondi et al., 1997). In this article, we report our finding that it generated novel fusion genes *ETV6/FRK* and *FRK/ETV6* in a case of AML. FRK belongs to a family of SRC kinases, as at the amino acid level, it has the highest homology, 50%, with FYN (Cance et al., 1994; Lee et al., 1994). Although several tyrosine kinase (TK) genes have been identified as fusion partners of *ETV6* (Golub et al., 1994; Papadopoulous et al., 1995; Lacronique et al., 1997; Peeters et al., 1997; Cazzaniga et al., 1999; Eguchi et al., 1999; Iijima et al., 2000; Kuno et al., 2001), this is the first report of a SRC-family tyrosine kinase gene being fused with *ETV6* and structurally altered in human cancers. In the resultant ETV6/FRK fusion protein, the entire PNT oligomerization domain of ETV6 and the kinase domain of FRK are fused in frame. We demonstrated that this ETV6/FRK fusion protein constitutively underwent autophosphorylation on its tyrosine residues. ETV6/FRK had elevated kinase activity compared to that in wild-type FRK. ETV6/FRK showed transforming activities in two cell lines, Ba/F3 and NIH3T3, indicating that ETV6/FRK is a dominant transforming oncoprotein. The kinase-inactive mutant ETV6/FRK(K262R) transformed neither of these two cell lines, indicating that the kinase activity of ETV6/FRK was essential for transformation. The reciprocal fusion protein FRK/ETV6, whose mRNA also was transcribed in the patient sample, did not have transforming activity. These data strongly suggest that the elevated kinase activity of the ETV6/FRK fusion protein directly contributes to the pathogenesis of leukemia with a t(6;12)(q21;p13).

Although activated variants of the SRC family kinases show transforming activities (Parker et al., 1984; Cartwright et al., 1987), the *SRC* and its family of genes rarely have been reported as being mutated or structurally altered in primary human tumors. Irby et al. (1999) reported that 12% of advanced human colon cancers in the United States had a truncating mutation at codon 531 of the *SRC* gene and that the mutation elevated kinase activity and promoted the potential for malignancy. However, three subsequent large-scale studies on advanced colorectal cancers in Japanese, northern European, Chinese, and Italian patients failed to detect the mutation (Daigo et al., 1999; Wang et al., 2000; Laghi et al., 2001), making the

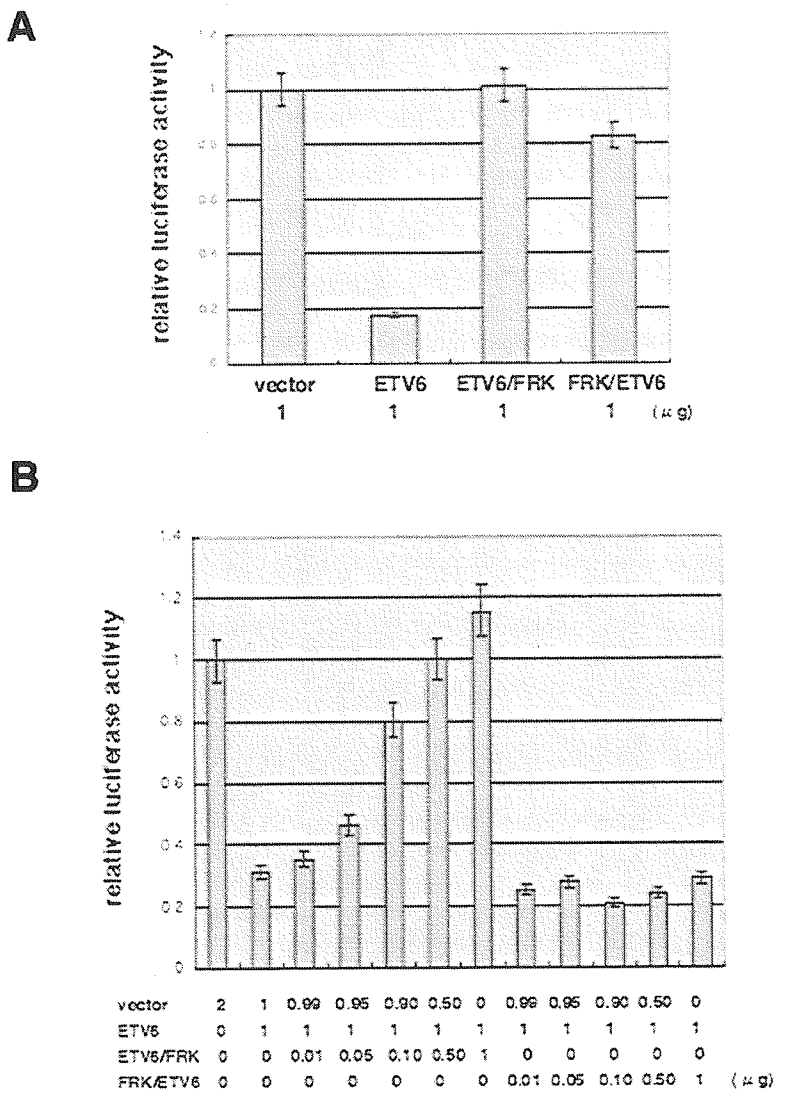

Figure 5. ETV6/FRK is a dominant-negative regulator of ETV6-mediated transcriptional repression in HeLa cells. (A) HeLa cells were transfected with 1 μg of (EBS)3tkLuc reporter plasmid along with 1 μg of the indicated expression vector. Bars show relative luciferase activities to the level when a control plasmid pME18S-neo was cotransfected with the corresponding reporter plasmid, and they present average results of duplicate experiments. (B) HeLa cells were transfected with 1 μg of (EBS)3tkLuc reporter plasmid along with 1 μg of pME-18S-neo-FLAG-ETV6 expression vector together with indicated amounts of pME18S-neo-FLAG-ETV6/FRK or pME18S-neo-FLAG-FRK/ETV6 expression vector. The results are presented as relative luciferase activities.

importance of this mutation controversial. In hematopoietic malignancies, two human T-cell acute lymphoblastic leukemia cell lines have been shown to have rearrangement of *LCK*, a SRC-family kinase gene (Tycko et al., 1991; Wright et al., 1994). In these two cell lines, HSB-2 and SUP-T12, the upstream promoter of the *LCK* gene was juxtaposed to the *TCRB* locus without any accompanying large structural abnormality of the LCK protein. *LCK* mRNA was elevated in the two cell lines (Tycko et al., 1991), and the HSB-2 cell line was later shown to carry several activating point mutations in the *LCK* gene (Wright et al., 1994), indicating that overexpression and/or activation of the LCK kinase would lead to cell transformation. On the other hand, the involvement of SRC family members in primary leukemia has not been reported previously. In this study, we showed that the structural abnormality of an SRC-like kinase gene, *FRK*, through translocation with *ETV6* can directly contribute to leukemogenesis through activation of the altered tyrosine kinase. In addition to the analysis of the current case with a t(6;12), we also performed a mutation analysis of the *FRK* gene in 20 hematopoietic cell lines but failed to detect activating mutations or structural abnormalities (data not shown). Thus, it is currently unclear whether FRK could be activated through other mechanisms such as activating mutations or translocations with other partner gene(s), although more intensive analyses may be required.

Two mechanisms could contribute to the constitutive activation of the ETV6/FRK kinase. First, in the ETV6/FRK fusion protein, the SH3 and SH2 domains of FRK are lost or disrupted, respec-

tively. Both the SH2 and SH3 domains are required to maintain the SRC family kinases in an inactive state: the SH2 domain binds to the C-terminal tyrosine residue in a phosphorylation-dependent manner, and the SH3 domain interacts with a short polyproline type II helix located between the SH2 domain and the kinase domain (Schindler et al., 1999; Xu et al., 1999; Young et al., 2001). These intramolecular interactions are believed to lock the molecule in a closed, inactive state, resulting in repression of kinase activity. In this regard, disruption of this closed conformation would activate the SRC family kinases and lead to cell transformation. In fact, some deletions or mutations in either the SH2 or the SH3 domain of SRC have been shown to activate its catalytic and/or transforming activities (Hirai and Varmus, 1990). Thus, the disruption of the SH3 and SH2 domains in ETV6/FRK may contribute to deregulation of kinase activity. Secondly, in the ETV6/FRK fusion protein, the entire PNT domain of ETV6 is fused to the kinase domain of FRK. As is the case with other ETV6/TK fusion proteins (Carroll et al., 1996; Golub et al., 1996; Jousset et al., 1997), the PNT domain would force dimerization of the ETV6/FRK protein and lead to constitutive tyrosine autophosphorylation and activation of the ETV6/FRK kinase.

The downstream signaling pathway mediated by ETV6/FRK still remains to be elucidated. The wild type FRK is expressed primarily in epithelial tissues (Cance et al., 1994), but also weakly in various hematopoietic cell line (data not shown). However, its functions or downstream signaling pathways remain largely unknown, especially in hematopoietic systems. The only known candidate endogenous downstream component of FRK is the SH2-domain adaptor protein SHB. According to recent reports, GTK, a rodent homologue of FRK, induces neurite outgrowth in PC12 cells and insulin stimulated signaling pathways in pancreatic insulin-producing cells via SHB (Anneren et al., 2000; Anneren and Welsh, 2002). In the present study, however, immunoblotting analysis failed to detect expression of the SHB protein in ETV6/FRK-expressing cells (data not shown). Thus, involvement of SHB in transformation by ETV6/FRK remains unclear. We also tested the phosphorylation status of several signaling molecules, including signal transducer and activator of transcription (STAT1, STAT3, STAT5, STAT6, extracellular signal-regulated kinase 1/2 (ERK1/2), P38 mitogen-activated protein kinase (P38 MAPK), phosphatidylinositol 3-kinase (PI3K), and phospholipase C (PLC)-gamma, in ETV6/FRK-expressing cells. However, we failed to detect any aberrant phosphorylation of these molecules in ETV6/FRK-expressing cells in comparison to FRK-expressing cells (data not shown). Future identification of the target substrate of ETV6/FRK might provide a novel insight into the mechanism of ETV6/FRK-induced transformation as well as of wild-type FRK-mediated signal transduction.

Finally, we demonstrated that ETV6/FRK had a dominant-negative effect over ETV6-mediated transcriptional repression. Because ETV6/FRK retains the PNT oligomerization domain of ETV6, ETV6/FRK may interfere with the transcriptional repression activity of ETV6 by heterodimerizing with wild-type ETV6. Our results indicate that ETV6/FRK is a novel oncoprotein with dual functions: deregulated tyrosine kinase activity and a dominant-negative modulation of transcriptional repression by ETV6. Because wild-type ETV6 appears to have tumor-suppressive activity (Romparey et al., 2000), its suppression by ETV6/FRK also could contribute to oncogenesis. It may be possible that ETV6/FRK can contribute to oncogenesis through two independent mechanisms: activation of the ETV6/FRK tyrosine kinase, which would lead to aberrant stimulation of the downstream signaling pathway, and inhibition of the tumor-suppressive functions of ETV6. This model suggests potential strategies for reversion of transformation by ETV6/FRK. Because the kinase-inactive mutant of ETV6/FRK is nontransforming, a specific inhibitor of the SRC family kinases may inhibit transformation by ETV6/FRK. Alternatively, overexpression of wild-type ETV6 also would interfere with the ability of ETV6/FRK to transform cells. Further experiments will explore these possibilities.

ACKNOWLEDGMENTS

We thank Dr. Kinuko Mitani for the gift of a full-length human *ETV6* cDNA and the (EBS)3t-kLuc reporter. We also thank Dr. Peter Marynen for providing cosmid probes 179A6, 50F4, 2G8, 184C4, and 88A9. Hisamaru Hirai died suddenly on August 23, 2003. His students, fellows, and colleagues will greatly miss his energetic leadership in the field of hematology. We dedicate this article to his memory.

REFERENCES

Anneren C, Welsh M. 2002. GTK tyrosine kinase-induced alteration of IRS-protein signalling in insulin producing cells. Mol Med 8:705–713.

Anneren C, Reedquist KA, Bos JL, Welsh M. 2000. GTK, a Src-related tyrosine kinase, induces nerve growth factor-independent neurite outgrowth in PC12 cells through activation of the Rap1 pathway. Relationship to Shb tyrosine phosphorylation and elevated levels of focal adhesion kinase. J Biol Chem 275:29153–29161.

Bolen JB, Veillette A, Schwartz AM, DeSeau V, Rosen N. 1987. Activation of pp60c-src protein kinase activity in human colon carcinoma. Proc Natl Acad Sci USA 84:2251–2255.

Brown MT, Cooper JA. 1996. Regulation, substrates and functions of src. Biochim Biophys Acta 1287:121–149.

Cance WG, Craven RJ, Bergman M, Xu L, Alitalo K, Liu ET. 1994. Rak, a novel nuclear tyrosine kinase expressed in epithelial cells. Growth Differ 5:1347–1355.

Carroll M, Tomasson MH, Barker GF, Golub TR, Gilliland DG. 1996. The TEL platelet-derived growth factor receptor (PDGFR) fusion in chronic myelomonocytic leukemia is a transforming protein that self-associates and activates PDGFR kinase-dependent signaling pathways. Proc Natl Acad Sci USA 93:14845–14850.

Cartwright CA, Eckhart W, Simon S, Kaplan PL. 1987. Cell transformation by pp60c-src mutated in the carboxy-terminal regulatory domain. Cell 49:83–91.

Cazzaniga G, Tosi S, Aloisi A, Giudici G, Daniotti M, Pioltelli P, Kearney L, Biondi A. 1999. The tyrosine kinase Abl-related gene ARG is fused to ETV6 in an AML-M4Eo patient with a t(1;12)(q25;p13): molecular cloning of both reciprocal transcripts. Blood 94:4370–4373.

Daigo Y, Furukawa Y, Kawasoe T, Ishiguro H, Fujita M, Sugai S, Nakamori S, Liefers GJ, Tollenaar RA, van de Velde CJ, Nakamura Y. 1999. Absence of genetic alteration at codon 531 of the human c-*src* gene in 479 advanced colorectal cancers from Japanese and Caucasian patients. Cancer Res 59:4222–4224.

Eguchi M, Eguchi-Ishimae M, Tojo A, Morishita K, Suzuki K, Sato Y, Kudoh S, Tanaka K, Setoyama M, Nagamura F, Asano S, Kamada N. 1999. Fusion of ETV6 to neurotrophin-3 receptor TRKC in acute myeloid leukemia with t(12;15)(p13;q25). Blood 93:1355–1363.

Golub TR, Barker GF, Lovett M, Gilliland DG. 1994. Fusion of PDGF receptor to a novel ets-like gene, tel, in chronic myelomonocytic leukemia with t(5;12) chromosomal translocation. Cell 77:307–316.

Golub TR, Goga A, Barker GF, Afar DE, McLaughlin J, Bohlander SK, Rowley JD, Witte ON, Gilliland DG. 1996. Oligomerization of the ABL tyrosine kinase by the Ets protein TEL in human leukemia. Mol Cell Biol 16:4107–4116.

Golub TR, Barker GF, Stegmaier K, Gilliland DG. 1997. The TEL gene contributes to the pathogenesis of myeloid and lymphoid leukemias by diverse molecular genetic mechanisms. Curr Top Microbiol Immunol 220:67–79.

Hayashi Y, Raimondi SC, Look AT, Behm FG, Kitchingman GR, Pui CH, Rivera GK, Williams DL. 1990. Abnormalities of the long arm of chromosome 6 in childhood acute lymphoblastic leukemia. Blood 76:1626–1630.

Hirai H, Varmus HE. 1990. Site-directed mutagenesis of the SH2- and SH3-coding domains of c-src produces varied phenotypes, including oncogenic activation of p60c-src. Mol Cell Biol 10:1307–1318.

Hu Y, Liu Y, Pelletier S, Buchdunger E, Warmuth M, Fabbro D, Hallek M, Van Etten RA, Li S. 2004. Requirement of Src kinases Lyn, Hck and Fgr for BCR-ABL1-induced B-lymphoblastic leukemia but not chronic myeloid leukemia. Nat Genet 36:453–461.

Iijima Y, Ito T, Oikawa T, Eguchi M, Eguchi-Ishimae M, Kamada N, Kishi K, Asano S, Sakaki Y, Sato Y. 2000. A new ETV6/TEL partner gene, ARG (ABL-related gene or ABL2), identified in an AML-M3 cell line with a t(1;12)(q25;p13) translocation. Blood 95:2126–2131.

Irby RB, Mao W, Coppola D, Kang J, Loubeau JM, Trudeau W, Karl R, Fujita DJ, Jove R, Yeatman TJ. 1999. Activating *SRC* mutation in a subset of advanced human colon cancers. Nat Genet 21:187–190.

Jousset C, Carron C, Boureux A, Quang CT, Oury C, Dusanter-Fourt I, Charon M, Levin J, Bernard O, Ghysdael J. 1997. A domain of TEL conserved in a subset of ETS proteins defines a specific oligomerization interface essential to the mitogenic properties of the TEL-PDGFR oncoprotein. EMBO J 16:69–82.

Katz JA, Taylor LD, Carroll A, Elder FFB, Mahoney DH. 1991. Cytogenetic features of childhood acute lymphoblastic leukemia: a concordance study and a pediatric oncology group study. Cancer Genet Cytogenet 55:249–256.

Kuno Y, Abe A, Emi N, Iida M, Yokozawa T, Towatari M, Tanimoto M, Saito H. 2001. Constitutive kinase activation of the TEL-Syk fusion gene in myelodysplastic syndrome with t(9;12)(q22;p12). Blood 97:1050–1055.

Kurokawa M, Tanaka T, Tanaka K, Ogawa S, Mitani K, Yazaki Y, Hirai H. 1996. Overexpression of the AML1 proto-oncoprotein in NIH3T3 cells leads to neoplastic transformation depending on the DNA-binding and transactivational potencies. Oncogene 12:883–892.

Lacronique V, Boureux A, Valle VD, Poirel H, Quang CT, Mauchauffe M, Berthou C, Lessard M, Berger R, Ghysdael J, Bernard OA. 1997. A TEL-JAK2 fusion protein with constitutive kinase activity in human leukemia. Science 278:1309–1312.

Laghi L, Bianchi P, Orbetegli O, Gennari L, Roncalli M, Malesci A. 2001. Lack of mutation at codon 531 of *SRC* in advanced colorectal cancers from Italian patients. Br J Cancer 84:196–198.

Lee J, Wang Z, Luoh SM, Wood WI, Scadden DT. 1994. Cloning of FRK/RAK, a novel human intracellular SRC-like tyrosine kinase-encoding gene. Gene 138:247–251.

Lopez RG, Carron C, Oury C, Gardellin P, Bernard O, Ghysdael J. 1999. TEL is a sequence-specific transcriptional repressor. J Biol Chem 274:30132–30138.

Maki K, Mitani K, Yamagata T, Kurokawa M, Kanda Y, Yazaki Y, Hirai H. 1999. Transcriptional inhibition of p53 by the MLL/MEN chimeric protein found in myeloid leukemia. Blood 93:3216–3224.

Ogawa S, Kurokawa M, Tanaka T, Mitani K, Inazawa J, Hangaishi A, Tanaka K, Matsuo Y, Minowada J, Tsubota T, Yazaki Y, Hirai H. 1996. Structurally altered Evi-1 protein generated in the 3q21q26 syndrome. Oncogene 13:183–191.

Ottenhoff-Kalff AE, Rijksen G, van Beurden EA, Hennipman A, Michels AA, Staal GE. 1992. Characterization of protein tyrosine kinases from human breast cancer: involvement of the c-src oncogene product. Cancer Res 52:4773–4778.

Papadopoulos P, Ridge SA, Boucher CA, Stocking C, Wiedemann LM. 1995. The novel activation of ABL by fusion to an ets-related gene, TEL. Cancer Res 55:34–38.

Parker RC, Varmus HE, Bishop JM. 1984. Expression of v-src and chicken c-src in rat cells demonstrates qualitative differences between pp60v-src and pp60c-src. Cell 37:131–139.

Peeters P, Raynaud SD, Cools J, Wlodarska I, Grosgeorge J, Philip P, Monpoux F, Van Rompaey L, Baens M, Van den Berghe H, Marynen P. 1997. Fusion of TEL, the ETS-variant gene 6 (ETV6), to the receptor-associated kinase JAK2 as a result of t(9;12) in a lymphoid and t(9;15;12) in a myeloid leukemia. Blood 90:2535–2540.

Pinkel D, Straume T, Gray JW. 1986. Cytogenetic analysis using quantitative, high-sensitivity, fluorescence hybridization. Proc Natl Acad Sci USA 83:2934–2938.

Raimondi SC, Shurtleff SA, Downing JR, Rubnitz J, Mathew S, Hancock M, Pui CH, Rivera GK, Grosveld GC, Behm FG. 1997. 12p abnormalities and the TEL gene (ETV6) in childhood acute lymphoblastic leukemia. Blood 90:4559–4566.

Rompaey LV, Potter M, Adams C, Grosveld G. 2000. Tel induces a G1 arrest and suppresses Ras-induced transformation. Oncogene 29:5244–5250.

Schindler T, Sicheri F, Pico A, Gazit A, Levitzki A, Kuriyan J. 1999. Crystal structure of Hck in complex with a Src family-selective tyrosine kinase inhibitor. Mol Cell 3:639–648.

Talamonti MS, Roh MS, Curley SA, Gallick GE. 1993. Increase in activity and level of pp60c-src in progressive stages of human colorectal cancer. J Clin Invest 91:53–60.

Tycko B, Smith SD, Sklar J. 1991. Chromosomal translocations joining LCK and TCRB loci in human T cell leukemia. J Exp Med 174:867–873.

Waga K, Nakamura Y, Maki K, Arai H, Yamagata T, Sasaki K, Kurokawa M, Hirai H, Mitani K. 2003. Leukemia-related transcription factor TEL accelerates differentiation of Friend erythroleukemia cells. Oncogene 22:59–68.

Wang NM, Yeh KT, Tsai CH, Chen SJ, Chang JG. 2000. No evidence of correlation between mutation at codon 531 of src and the risk of colon cancer in Chinese. Cancer Lett 150:201–204.

Wright DD, Sefton BM, Kamps MP. 1994. Oncogenic activation of the Lck protein accompanies translocation of the LCK gene in the human HSB2 T-cell leukemia. Mol Cell Biol 14:2429–2437.

Xu W, Doshi A, Lei M, Eck MJ, Harrison SC. 1999. Crystal structures of c-Src reveal features of its autoinhibitory mechanism. Mol Cell 3:629–638.

Young MA, Gonfloni S, Superti-Furga G, Roux B, Kuriyan J. 2001. Dynamic coupling between the SH2 and SH3 domains of c-Src and Hck underlies their inactivation by C-terminal tyrosine phosphorylation. Cell 105:115–126.